

PAPER • OPEN ACCESS

## Nuclear physics aspects of neutron capture and $\beta$ -decay rates in stellar environment

To cite this article: A Mengoni 2020 *J. Phys.: Conf. Ser.* **1668** 012027

View the [article online](#) for updates and enhancements.



**ECS** **240th ECS Meeting**  
Digital Meeting, Oct 10-14, 2021  
**We are going fully digital!**  
Attendees register for free!  
**REGISTER NOW**

# Nuclear physics aspects of neutron capture and $\beta$ -decay rates in stellar environment

A Mengoni<sup>1,2</sup>

<sup>1</sup>ENEA, Agenzia Nazionale per la nuove Tecnologie, l'Energia e lo Sviluppo Economico Sostenibile, Bologna, Italy

<sup>2</sup>INFN, Istituto Nazionale di Fisica Nucleare, Sezione di Bologna, Italy

E-mail: [alberto.mengoni@enea.it](mailto:alberto.mengoni@enea.it)

**Abstract.** Under stellar conditions, nuclear reaction rates are different from those measured in laboratory. A notable example of this situation is the stellar rate for neutron capture, when nuclear excited states can be thermally populated and the capture process can proceed not only for the ground state but also from nuclear excited levels. While the composite nucleus of the capture process is the same, different excited compound states can be populated from different target nuclear levels. In addition, inelastic scattering channels can be open for these states, in which the neutron is scattered out with kinetic energy higher than kinetic energy of the entrance channel (the so-called super-elastic scattering). An additional example of the modification of stellar rates with respect to laboratory rates is provided by the  $\beta$ -decay. Here, the different degree of ionization of the nuclei involved imply a modification of the phase-space factor in the decay probability. In addition, here again, excited parent decaying states can be populated in a stellar plasma and additional transitions, with different degrees of forbidness, become possible. A dramatic change in the  $\beta$ -decay rates under stellar conditions have been predicted and observed in a number of cases. A review of these two rates evaluations, from the theoretical point of view as well as from the perspectives of their experimental determination is presented with some relevant examples for both, neutron capture and  $\beta$ -decay processes.

## 1. Introduction

The rates for reactions taking place in stellar environment are different with respect to rates measured in laboratory conditions. In dense, hot plasmas in which the nuclear reactions take place, nuclei participating in the reaction processes can be thermally excited and therefore, the reaction process can be completely different from that induced in laboratory, where target nuclei used for reaction cross section measurement can only be on their ground states. In general, for any reaction  $(a, b)$ , the cross section in stellar environment can be written as

$$\sigma^*(a, b) = p_0\sigma_0(a, b) + p_1\sigma_1(a, b) + \dots + p_N\sigma_N(a, b) \quad (1)$$

where  $p_i$  are the probabilities for populating any nuclear state  $i \equiv \{E, J\}$ ,  $i = 1, \dots, N$  with total angular momentum  $J$  and excitation energy  $E$  at temperature  $kT$

$$p_i = \frac{(2J_i + 1)e^{-E_i/kT}}{\sum_{i=1}^N (2J_i + 1)e^{-E_i/kT}}. \quad (2)$$



In laboratory, only  $\sigma_0(a, b) \equiv \sigma_{LAB}(a, b)$  can be measured. The various  $\sigma_i(a, b)$  must be evaluated from nuclear reaction theory. For example, for medium-mass and heavy nuclei, nuclear reactions can be modelled in the framework of the Hauser-Feshbach statistical model (HFSSM) theory. In the particular case of neutron capture, the ratio between the stellar and the laboratory cross sections is usually referred to as the "stellar enhancement factor", SEF  $\equiv \sigma^*(n, \gamma)/\sigma_0(n, \gamma)$ .

In the case of  $\beta$ -decay, a similar relation as in Equation 1 holds for the decay rate

$$\lambda^*(\beta) = p_0\lambda_0(\beta) + p_1\lambda_1(\beta) + \dots + p_N\lambda_N(\beta) \quad (3)$$

where  $\beta = \beta^-, \beta^+$  or  $EC$ .

A theory for the evaluation of  $\beta$ -decay rates in stellar environment has been elaborated in the work of Kohji Takahashi and Koichi Yokoi [4, 5]. It can be summarized (all the details are given in the references) in the following. The decay rate is given by

$$\lambda = \frac{2\pi}{\hbar} |H|^2 \omega(p_e) \quad (4)$$

where  $H$  indicates the matrix elements of the nuclear transition and  $\omega(p_e)$  the phase volume which depends on the emitted/captured lepton momentum  $p_e$  and it is given by

$$\omega(p_e^{max}) = \int_0^\infty |\Psi_e(R)|^2 (E_{max} - E_e)^2 p_e^2 dp_e \quad (5)$$

where  $E$  is the electron/positron kinetic energy and  $\Psi(R)$  its wave function at the nuclear radius  $R$ . The stellar rate is then related to the comparative half-life  $ft$  by

$$\lambda^* = \left[ \frac{\ln 2}{ft} \right] f^* \quad (6)$$

with

$$f^* = \int_0^{W_{max}} (W^2 - 1)^{1/2} W q^2 F_0 S f_d dW. \quad (7)$$

Here,  $W = 1 + Q/m_e c^2$  and  $q = W_{max} - W$ . The spectral function  $S$  is a linear combination of electron/positron wave functions and  $F_0$  the Fermi function as cited in [4], together with

$$f_d = \frac{1}{1 - e^{-\beta(W-1)+\eta}}, \quad \beta = \frac{m_e c^2}{kT} \quad (8)$$

and  $\eta$  the electron degeneracy. All the relations above depend on the  $Q$ -value for the transition which, in turn, depend on the energy difference of the nuclear initial and final states, as well as on the total binding energies of bound electrons in the ionized atomic ground-states and of their excited ionic states. The final stellar decay rates  $\lambda^*$  have to be weighted over the population probability distribution of the atomic ion states for a given temperature and electron density, which define the thermodynamical condition of the stellar plasma under consideration.

A major difference between the reaction and the  $\beta$ -decay cases is that, while the various  $\sigma_i(a, b)$  can be different but of the same order of magnitude, the decay rates  $\lambda_i(\beta)$  can be different by several orders of magnitude. In the following examples, this condition will be shown.

## 2. Example of a stellar neutron capture rate

As an example of evaluation of a stellar rate, we consider here the case of the  $^{186}\text{Os}(n, \gamma)^{187}\text{Os}$  and of the  $^{187}\text{Os}(n, \gamma)^{188}\text{Os}$  reactions. The cross sections for these reactions are relevant for the Re/Os nuclear cosmochronometer [1]. The laboratory cross sections have been measured (see

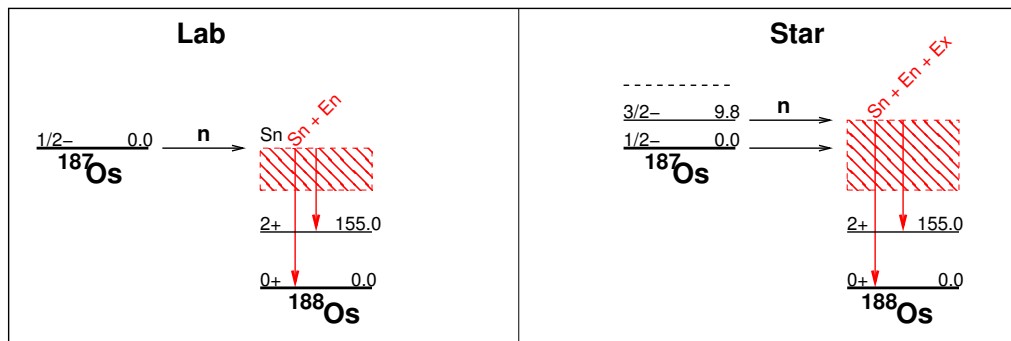


**Figure 1.** Schematic view of the neutron capture process on  $^{187}\text{Os}$  in laboratory (left panel) and in a hot stellar environment (right). Only the first excited state in  $^{187}\text{Os}$  is shown explicitly. Excitation energies are in units of keV.

[2] and references therein for previous measurements), from which HFSM calculations can be tuned. The particular case of the  $^{187}\text{Os}(n, \gamma)^{188}\text{Os}$  reaction is indicated in the Figure 1. At a typical temperature of  $kT = 30$  keV, the ground state of  $^{187}\text{Os}$  is populated by 33%, while the first excited state at 9.8 keV is populated at 47% and the remaining states by 20%. The capture cross sections for these target states can be calculated using HFSM, with parameters tuned to reproduce the laboratory cross section  $\sigma_0(n, \gamma)$ . A stellar enhancement factor  $\text{SEF} = 1.29 \pm 0.04$  has been evaluated, including the super-elastic channel which is open for nuclear excited states. The relatively small uncertainty on the SEF is due to the fact that, if the compound nucleus reaction process is assumed, the compound system is always the same for any of the target states and, therefore, the de-excitation process is the same, regardless of the target nuclear state from which it is formed. In addition, considering that the SEF depends only on cross section ratios (see Equation 1), a relatively small uncertainty of the order of 4% has been associated with the evaluated stellar enhancement factor for this capture reaction.

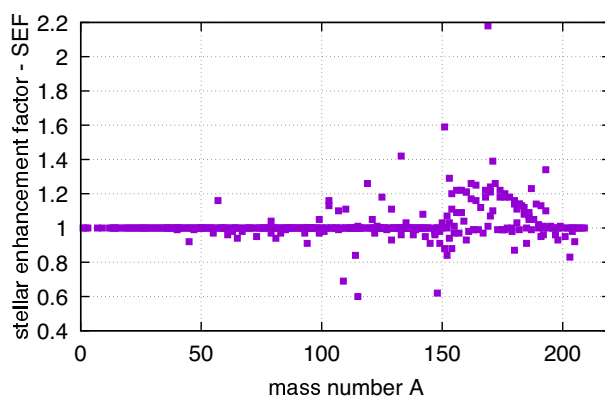


**Figure 2.** A systematics of stellar enhancement factors, as reported in the KADONIS database [3]

In order to consider globally the effect of thermal population on capture rates, the systematics of SEF's reported in the KADONIS database [3] is show in Figure 2. It can be seen that the range of variation of the SEF is, for the whole mass range covered, within a factor of  $\approx 2$ . It is clear that the effect of thermalization of nuclear excited states has important consequences on the detailed modeling of the nucleosynthesis of heavy elements, in particular on the relative contribution of *slow* and *rapid* neutron capture processes. In the particular case considered here, the effect of thermalization of nuclear states implies an increase in the estimated time-duration

of the nucleosynthesis over the galactic age of 1.7 Gyr [2].

### 3. Example of a stellar $\beta$ -decay rate

As an example of application of the Takahashi & Yokoi model (TYM) [4], we consider here the case of the  $\beta$ -decay of  $^{176}\text{Lu}$ . The laboratory half-life of the  $J^\pi = 7^-$  ground state is  $t_{1/2} = 37.6$  Gyr, for 1st-forbidden non-unique transitions leading mostly (99.6%) to the  $J^\pi = 6^+$  excited state in  $^{176}\text{Hf}$ . The question of the enhanced rate at high temperatures due to the presence of the  $J^\pi = 1^-$  isomer at 122.8 KeV which has an half-life of only 3.66 hours for has been investigated in the past [6].

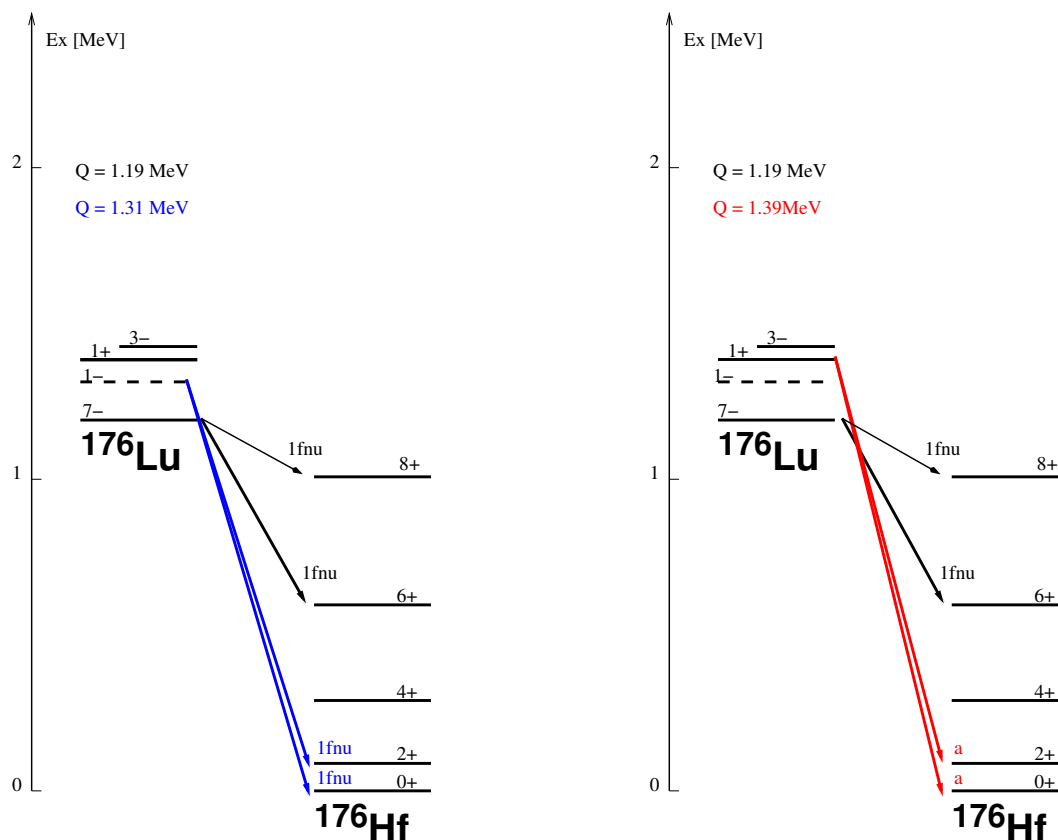


**Figure 3.** Decay scheme of  $^{176}\text{Lu}$  ground state ( $t_{1/2} = 37.6$  Gyr) and isomer at 123 keV ( $t_{1/2} = 3.7$  hr) through 1st-forbidden non-unique  $\beta^-$  transitions (left panel). Allowed transitions from the  $1^+$  state at 194 keV are indicated in the right panel.

In addition to the isomer, which as the ground state decays by 1st-forbidden non-unique transitions to the ground and 1st excited states in  $^{176}\text{Hf}$ , the  $1^+$  state decays by allowed transitions to the same states. This situation is shown schematically in Figure 3.

The calculations have been performed here for a plasma with electron density  $n_e = 10^{26} \text{ cm}^{-3}$ , assuming local thermodynamical equilibrium (LTE). From the LTE conditions, the population probability for ion charge distributions can be easily derived and the related Q-values generalized to include the total binding energies of bound electrons. In the specific case considered here, the effect on the decay rate is negligible. The LTE condition can be, in principle, relaxed and the TYM extended to non-local thermodynamical equilibrium conditions (NLTE). The dramatic effect of electron configurations on the  $\beta$ -decay rate has been demonstrated in the case of the

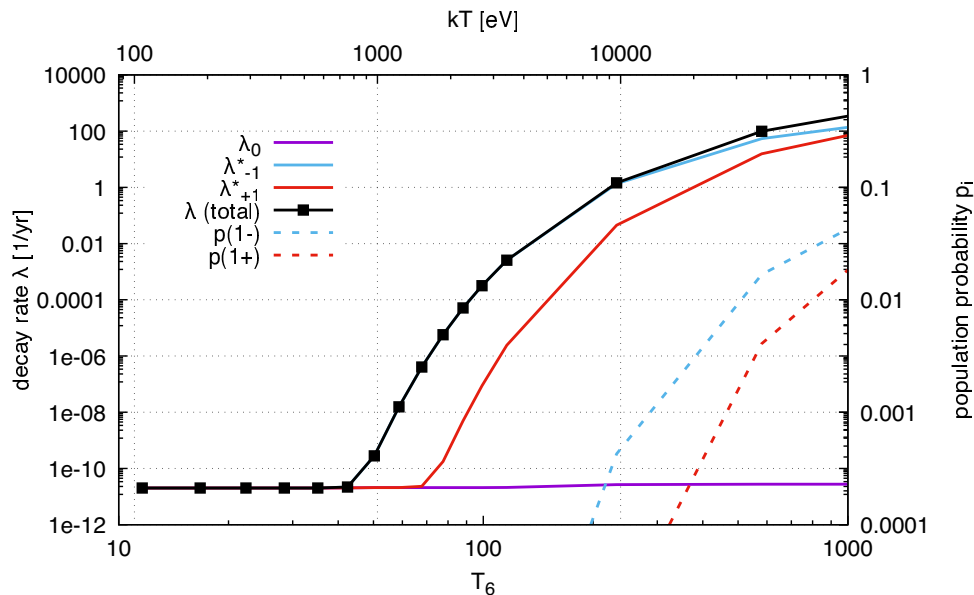


**Figure 4.** Evolution of the  $\beta$ -decay rate with temperature for the  $J^\pi = 7^-$  ground state ( $\lambda_0$ ), and of the stellar rates when including the  $1^-$  isomer at 123 keV ( $\lambda_{1-}^*$ ) and the  $1^+$  state at 195 keV ( $\lambda_{1+}^*$ ) of  $^{176}\text{Lu}$ . The stellar rates are calculated for a plasma with electron density  $n_e = 10^{26} \text{ cm}^{-3}$ .

$^{187}\text{Re}(\beta^-)^{187}\text{Os}$  in the work performed at GSI [7], confirming the predictions of the TYM, at least for the extreme case of fully ionized atoms.

The results of the present calculations are shown in Figure 4. Even though the population probability of the considered excited states is very low, their much faster decay rates makes a dramatic change in the related half-life, which decrease down to approximately one year at  $kT = 10 \text{ keV}$  and decreases further down at higher temperatures. To be noted as well is that even if the  $1^-$  isomer is not thermalized, the presence of the  $1^+$  state immediately above, makes the transition rate anyway much faster than the laboratory rate, at least for temperatures above a few keV.

#### 4. New developments in experimental studies of $\beta$ decay

The possibility to study  $\beta$ -decay rates in stellar environment is the main purpose of a new project initiated by the Italian National Institute for Nuclear Physics [8]. PANDORA ("Plasmas for Astrophysics, Nuclear Decays Observation and Radiation for Archaeometry") is based on a state-of-the-art magnetic trap confining energetic plasma aimed at studying the effect of high temperatures and electron densities on the decay rates of radioactive ions. In PANDORA, a new plasma heating methods will be explored, that will push forward the ion beam output, in terms of extracted intensity and charge states. In addition, advanced and optimized injection methods of ions in an ECR plasma will be experimented, with the aim to optimize their capture efficiency. An extended system of plasma diagnostic devices are planned to be installed, together with detection system for ion decay emitted radiation.

In PANDORA, a buffer plasma of He, O or Ar will be created, with densities up to  $10^{13} \text{ cm}^{-3}$ . The isotope to be measured will be directly fluxed (if gaseous) or vaporized by appropriate ovens inside the chamber and turned into a plasma-state. Relative abundances of buffer *vs.* isotope densities varies from 100:1 (if the isotope is in a metal state) to 3:1 (in case of gaseous

elements). The plasma is maintained in dynamical equilibrium by equalizing input fluxes of particles to losses from the magnetic confinement. Operative ECR frequency will be 18 GHz, with a maximum magnetic field of 2.4 Tesla. Additional parameters of the main device are being defined. With PANDORA, it will be possible to study, independently, the effect of electronic configurations at high electron densities, as well as the effects of nuclear thermalization at high temperatures on the decay rates of radioactive ions of interest in nuclear astrophysics.

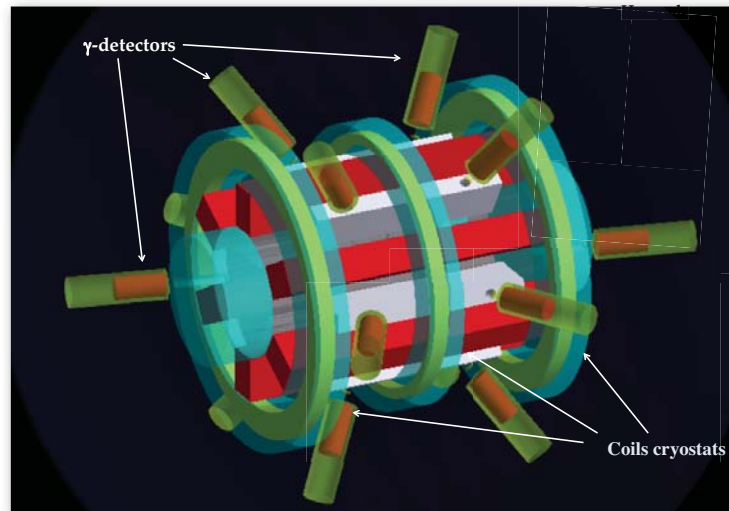


**Figure 5.** Schematic view of the PANDORA ion trap. A hybrid super/normal-conducting coil system is envisaged. In the simulated layout, external detectors for  $\gamma$ -ray detection are indicated. In the project design [8], several devices for plasma diagnostics will be installed, together with a radiation detection system to detect the injected ion decays.

## References

- [1] Clayton D D 1964, *ApJ* **139** 637
- [2] Mosconi M, K Fujii, Mengoni A *et al.* (The n\_TOF Collaboration) 2010, *Phys. Rev. C* **82** 015802  
Mosconi M, Heil M, Käppeler F, Plag R, and Mengoni A 2010, *Phys. Rev. C* **82** 015803  
Fujii K, Mosconi M, Mengoni A *et al.* (The n\_TOF Collaboration) 2010, *Phys. Rev. C* **82** 015804
- [3] Dillmann I, Plag R, Käppeler F, and Rauscher T 2009, Proceedings of the workshop *EFNUDAT - Scientific workshop on neutron measurements, theory and applications* held on 28-30 April 2009 at Geel, Belgium (see <http://kadonis.org>).
- [4] Takahashi K and Yokoi K 1983, *Nucl. Phys.* **A404** 578
- [5] Takahashi K and Yokoi K 1987, *Atomic Data Nuclear Data Tables* **36** 375
- [6] Klay N, Käppeler F, Beer H, and Schatz G 1991, *Phys. Rev. C* **44** 2839
- [7] Bosch F, *et al.* 1996, *Phys. Rev. Lett.* **76** 5190  
Litvinov Y and Bosch F 2011, *Rep. Progr. Phys.* **74** 016301
- [8] Mascali D *et al.* 2017, *Eur. Phys. Jour. A* **53** 145  
Mascali D *et al.* 2020, WOS Conf. Proceed., *10th European Summer School on Experimental Nuclear Astrophysics* (Catania, Italy, June 16 - 23, 2019), in press